Differential Displacement Kerma Cross Sections for Neutron Interactions in Si and GaAs

A. M. OUGOUAG, MEMBER, IEEE, J. G. WILLIAMS, MEMBER, IEEE, M. B. DANJAJI, S.-Y. YANG, AND J. L. MEASON, MEMBER, IEEE

Abstract—**The cross-section processing code NJOY has been modified to calculate flux-averaged partially integrated differential displacement kerma cross sections, or displacement kerma matrix elements, for neutron interactions. These, and total displacement kerma cross sections, have been calculated using ENDF/B-V and ENDL-84 data files for Si, Ga, and As. The displacement kerma matrices for Si and GaAs allow calculations of the distribution of displacement energy between displacement cascades.**

Introduction

DISPLACEMENT kerma cross sections are used to calculate the energy deposited in the form of displacement damage by neutron interactions. Damage caused by individual neutron interactions occurs along the tracks of recoiling charged particles, particularly at the ends of these tracks. The displacement kerma matrices, calculated in this work, enable one to calculate not only the total damage energy, but also the distribution of damage energy between charged particle cascades resulting from individual neutron interactions. This information is needed in order to account for damage effects that depend not only on the total displacement energy, but also on its distribution between discrete damage structures. Some examples of applications of such results, based on primary recoil atom (PKA) spectra, have been previously cited by Kirk and Greenwood [1], who presented damage energy distributions for Si, Ni, Nb, and Au irradiated in a particular reactor facility.

The calculations in this work have been performed with a modified version of the NJOY code [2], [3]. Displacement kerma cross sections for specified ranges of damage energy can be calculated using our modified version.

Review of Previous Work

Most predictions of the neutron-energy dependence of damage in semiconductors have been based on the assumption that the effects are a function only of the amount of nonionizing or displacement energy deposited (e.g., ASTM Standard E722 [4]). There are, however, some limitations in applying this assumption. These arise principally in two ways.

Displacement-induced defects include simple Frenkel pairs, other point defects created by diffusion and substitution processes, and complex stable-defect structures, which are likely to arise only in the highly disordered regions produced at the ends of heavy recoil tracks. Annealing treatments [5], [6] readily provide evidence of the different thermodynamic properties of defects from different types of irradiation (and hence of their different structures). Furthermore, the production of stable defects from the initial displaced atoms does not result in a one-to-one efficiency of stable defect production from displacements [7].

Different defect structures, in addition to having different efficiency for their formation, may also have different efficacy in producing macroscopic manifestations (''effects''). This is accounted for neither in the usual correlation of effects with displacements energy, nor in the Gossick [8] and Crawford [9] space-charge model, which does not take into account the distribution of cascade size. Van Lint *et al.* [10] have proposed that, in clusters of neutron-produced defects, it is not the number of defects but the area of the space-charge region that is responsible for electronic effects. The area does not scale linearly with the number of defects in the cascade. In fact, the effect of cascade size on excess-carrier lifetime scales differently from the effect on majority-carrier concentration and, therefore, the correct correlation parameter may be different for different semiconductor properties.

In spite of these arguments, in the case of silicon, extensive previous and current efforts have validated the assumption that damage effects on bipolar transistor gain, which depend primarily on minority carrier lifetime, are proportional to the energy deposited in the form of atomic displacements (for example, see [11]–[14]). In [12], Summers *et al.* refer to the agreement between their calculations and measurements as

> surprising when it is recalled that the energy deposition has been calculated only for the PKAs, that is none of the subsequent solid state effects such as channeling, damage cascades, or annealing have been considered.

They point out that their results are consistent with the findings of the Monte Carlo calculations (e.g., [15]–[17]) that subcascade size distributions are similar for a wide range of PKA energies. This is explained in [16] by the argument

Manuscript received July 24, 1989; revised June 26, 1990. This work was supported in part by the U.S. Army under contract no. DAAD07-87-K-0018.

A. M. Ougouag, J. G. Williams, M. B. Danjaji, and S.-Y. Yang are with the University of Illinois, Urbana-Champaign, IL 61801.

J. L. Meason is with the Nuclear Effects Laboratory, White Sands Missile Range, NM 88002.

IEEE Log Number 9038739.

0018-9499/90/1200-2219$01.00

that, in Si, PKA's of energy above 12 keV launch subcascades resembling those formed by less energetic PKA's, and that this occurs on a faster time scale than that associated with cascade collapse and annealing. Crucial to this argument is the assumption that subcascades behave as independent structures both in their annealing and in their electronic effects.

Pease *et al.* [18] have also compared carrier removal rates in Si with predictions based on damage energy deposition and found good correlations between results for a wide range of bombarding proton energies. Only at the highest proton energy, 175 MeV, was the correlation not good. The authors attributed this to a dosimetry problem, but the high-energy result may have significant implications for fast neutron damage in which the mean PKA energy is higher than for protons, even of 175 MeV.

In the case of gallium arsenide less calculational data on the structure of cascades are available, though PKA energy distributions following proton bombardment have been published by Hamm *et al.* [19] and by Farrell *et al.* [20]. The latter point out that gallium arsenide reactions deposit more energy (than Si reactions) in small sensitive volumes because of the higher linear energy transfer (LET) of the recoils.

Experimental evidence on the correlation of damage effect in GaAs with displacement damage energy has been presented by Luera *et al.* [13] for fast neutron bombardment and by Burke *et al.* [21] and Summers *et al.* [22] for proton bombardment. The latter also presented reanalyzed data of earlier authors [23], [24] using electrons and heavy ions. Luera *et al.* [13] suggested that the poor correlation between reactor neutron effects and 14-MeV neutron effects, which they observed for GaAs but not for Si, may be due to cluster or cascade size effects in GaAs. Summers *et al.* found a good correlation between displacement damage energy and effects except for 188-MeV protons, which produce more high-energy recoils than other particles included in the paper, but not so many as fast neutrons. They attributed the discrepancy to nonlocal energy deposition owing to the small dimensions of the test structures' sensitive volumes relative to the PKA ranges. They implied that a similar effect may explain the result of Luera *et al.* for neutrons, but this is not a plausible explanation in that case because of the relatively large thickness of the epitaxial layer on the Van der Pauw specimens used.

Theory

The computational results presented in this paper were obtained using a locally modified version of the NJOY cross-section processing code [2]. The modifications were introduced to provide an improved treatment of the emitted charged particles from (n, particle) and (n, n' particle) reactions and to compute the differential displacement kerma cross sections integrated over displacement energy groups. The theory underlying these changes is summarized as follows.

Emitted energetic charged particles as well as the recoil can produce displacement damage. The computational treatment of the emitted charged particles is formally similar to that of the recoils. If the energy of the charged particle is E_b, the corresponding energy contributing to displacement damage is computed as

$$E_{Db} = E_b L(E_b)$$

where $L(E_b)$ is the Robinson [25] version of the Lindhard [26] partition function for the particular charged particle in the material under consideration. Conservation of energy is assured by imposing that the emitted particle carries away the portion of the available energy not taken by the recoil; this also defines the particle energy distribution.

The damage due to one recoil (or one emitted charged particle) may be regarded as a single cascade. The size (or amount of damage) of a cascade can be characterized by the energy of the recoil atom (or charged particle) that causes it. The energy of the PKA causing the cascade can be used as a rough quantifier of the amount of damage the PKA will produce within the cascade, and hence of the "size" (in terms of damage) of the cascade. Some insight into the size distribution of cascades (i.e., the distribution of the amount of damage) can therefore be obtained from the energy distribution of the PKA's or that of the emitted particles. In the theory presented here, the distribution of damage due to PKA's as well as emitted charged particles is evaluated from their respective energy, energy distribution, and the appropriate Lindhard partition function. The resulting measure for the cascade size is the corresponding displacement kerma matrix element or differential kerma factor.

Let $K_D(E, E_D)\,dE_D$ be the differential displacement kerma cross section for neutron collisions, which result in displacement cascades with displacement energy between E_D and $E_D + dE_D$. In the NJOY code the quantity

$$\begin{aligned} K_D(E) &= \int_0^\infty K_D(E, E_D)\, dE_D \\ &= \sigma(E) \int_0^\infty E_R L(E_R) f(E, E_R)\, dE_R, \end{aligned} \quad (1)$$

where $f(E, E_R)$ is the energy distribution of the recoil, is computed and given as a function of the neutron energy E. NJOY was modified to allow the computation of the partially integrated quantities

$$^jK_D(E) = \int_{E_{Dj}}^{E_{Dj+1}} K_D(E, E_D)\, dE_D, \qquad j = 1, \cdots, J, \quad (2)$$

where the index j refers to the range $[E_{Dj}, E_{Dj+1}]$ of single cascade damage energy.

In practice $^jK_D(E)$ is computed within NJOY using integration over the recoil energy E_R (or one or more related variables), i.e.,

$$^jK_D(E) = \int_{E_{Rj}}^{E_{Rj+1}} K_D(E, E_R)\, dE_R, \qquad j = 1, \cdots, J, \quad (3)$$

where the limits E_{Rj+1} and E_{Rj} are obtained from the corresponding E_D values for every type of recoil or emitted charged particle. Finally, in order to arrive at the damage cascade size distribution, the various $^jK_D(E)$ estimates are summed over all the charged particles and/or reactions.

We propose to account for the effects of different cascade sizes described in the previous section by means of a parameter, which we shall call the damage macroeffectiveness and which we assume to be a function of the displacement energy expended in the formation of individual structures.

An observed effect F can be correlated to the displacement kerma via

$$F = \int_0^\infty \phi(E)\left[\int_0^\infty w(E_D)K_D(E, E_D)\, dE_D\right] dE \quad (4)$$

where $\phi(E)$ is the neutron flux density spectrum and where $w(E_D)$ is the continuous-energy macroeffectiveness factor. In multigroup form this is written

$$F = \sum_g \phi_g \sum_j w_j\, {}^jK_{Dg} \quad (5)$$

where the following definitions are used:

$$\phi_g = \int_{E_g}^{E_{g+1}} \phi(E) \quad dE, \quad (6)$$

$$^jK_{Dg} = 1/\phi_g \int_{E_g}^{E_{g+1}} \phi(E) \cdot\left[\int_{E_{Dj}}^{E_{Dj+1}} K_D(E, E_D)\, dE_D\right] dE, \quad (7)$$

and

$$w_j = \frac{F_{jm}}{\sum_g {}^jK_{Dg}} \quad (8)$$

where F_{jm} is the measured effect (i.e., the experimental response) attributable to cascades of damage energy in the range $[E_{Dj}, E_{Dj+1}]$ for the material under consideration in the neutron field $\phi(E)$. In practice F_{jm} may not be available for components of a given field $\phi(E)$ and it may be necessary to solve for the w_j factors using a linear system obtained using a number of fields.

The new approach presented here can be used to define a 1-MeV equivalent fluence as

$$\phi(\text{1-MeV}) = \frac{\int_0^\infty \phi(E)K'_D(E)\, dE}{K'_D(\text{1-MeV})}, \quad (9)$$

where

$$K'_D(E) = \int_0^\infty K_D(E, E_D)w(E_D)\, dE_D = \sum_j w_j\, {}^jK_D(E). \quad (10)$$

The $^jK_D(E)$ terms are computed in NJOY as an intermediate step in the computation of $^jK_{Dg}$.

This definition of the 1-MeV equivalent fluence is equivalent to the one in current use when the multigroup macroeffectiveness factors w_j are taken to be equal.

Results

The total displacement kerma cross sections for Si, Ga, and As were calculated using the modified version of NJOY87 and nuclear data files from ENDF/B-V and ENDL-84. Si and Ga evaluations are included in the general purpose file of ENDF/B-V in files MAT1314 and MAT1358, respectively. Arsenic is not included in the general purpose file because ENDF/B contains only an incomplete evaluation. The material MAT8302 of the Lawrence Livermore Library ENDL-84, available from the Radiation Shielding Information Center (RSIC) in ENDF/B-V format [27], was used for the As calculations. The two target atoms in GaAs have nearly the same mass and nearly the same displacement threshold energy. The displacement threshold energy E_d used for Ga and As was 10 eV. The data for the two target elements were simply averaged to obtain GaAs displacement kerma cross sections in units of electron volt barns per atom. For Si the value 25 eV was used for E_d.

Fig. 1 and Table I (presented in the Appendix) show the calculated total displacement kerma cross sections for Si and GaAs in the 620-group SAND group structure. The lengthy table is included in this paper in order to make these data available to users and owners of hardness testing facilities and to provide complete documentation of our results. The figure is similar to one by Luera *et al.*, for which tabulated data (Sandia data) were not printed [13]. Our Si data have been compared with a recent version of the Sandia data and agree with them to within 1% [14]. The GaAs data have not been compared. Fig. 2 shows the same data as Fig. 1 but on linear scales, which present the important higher energies more clearly. The GaAs values are similar to the Si values at 1 MeV but are about 50% larger at 14 MeV.

In Fig. 3 the calculated displacement kerma matrices for selected displacement energy ranges are shown for Si. These were computed in the same 620 neutron energy group structure. Displacement cascade energies E_D were represented in seven energy ranges from zero up to the maximum displacement energy that can be caused by a neutron of less than 18 MeV. The figure shows three of the displacement energy ranges corresponding to small, medium, and large cascade sizes. Damage energy ranges 1, 3, and 5 (as defined in the tables of the Appendix) are shown.

Data for the seven displacement energy ranges are shown in Table II in the Appendix, in which the neutron energy groups were condensed into multigroup form with the same group boundaries as those of the 37-group DNA group structure [28]. We believe that the 37-group representation is sufficient for these data, though we also have them in 620-group form. The fluence weighting function used for all the data presented here is a ^{235}U fission neutron spectrum joined to a 1/E spectrum at 100 keV, and joined to a Maxwellian thermal spectrum (300K) at 0.1 eV. This weighting is typical of light water reactor spectra and is different from that of the DNA 37 group structure, which uses strictly a 1/E joined to a 300K Maxwellian at 0.129 eV.

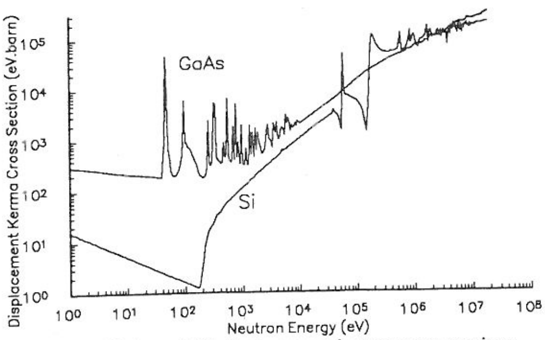

Fig. 1. GaAs and Si displacement kerma cross sections.

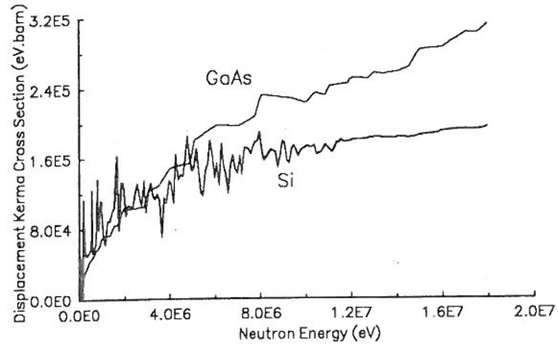

Fig. 2. GaAs and Si displacement kerma cross sections.

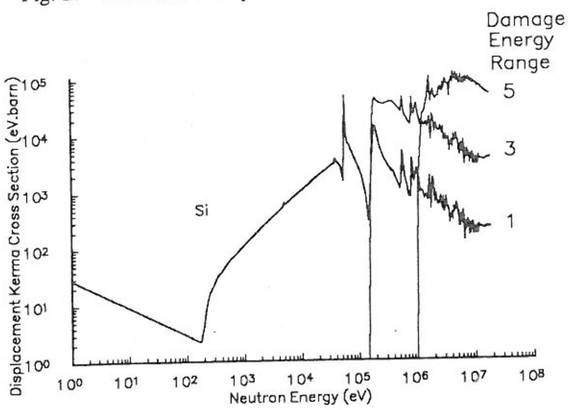

Fig. 3. Si displacement kerma matrix coefficients.

Table II contains the quantities ${}^jK_{Dg}$, which are defined in (7). These, when folded with any neutron energy spectrum ϕ_g tabulated in the DNA 37-group structure, may be used to obtain the distribution D_j ($j = 1, 2, \cdots J$) of the displacement damage energy between different cascade sizes:

$$D_j = \sum_g \phi_g {}^jK_{Dg}, \qquad j = 1, \cdots, J. \tag{11}$$

Displacement kerma matrix coefficients for GaAs are shown in Table III in the Appendix and in Fig. 4 for three selected ranges. The displacement energy ranges that were selected for GaAs are different from the ones used for Si because, on average, the recoil energies and the displacement energies are smaller for more massive target atoms. In order to allow them to be combined, the displacement energy ranges were chosen to be the same in the calculations for Ga and As. In all cases the global range was chosen to cover all possible causes of displacement damage.

Figs. 3 and 4 show that for both Si and GaAs, the larger cascades are produced predominantly by the highest energy neutrons. Small cascades (small displacement energy) are produced by neutrons of all energies, but especially by the lower-energy neutrons.

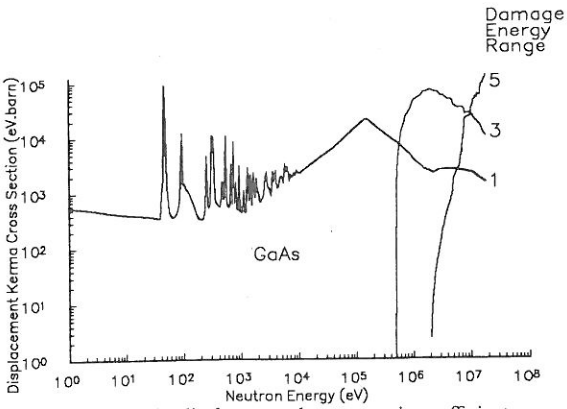

Fig. 4. GaAs displacement kerma matrix coefficients.

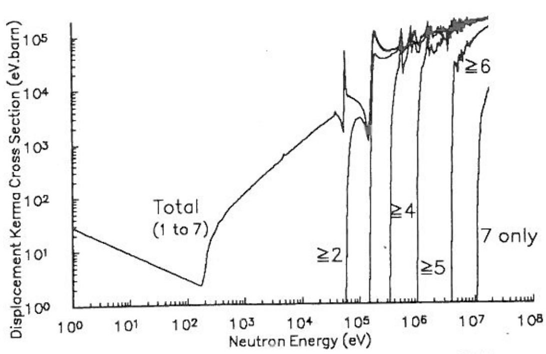

Fig. 5. Cumulative Si displacement kerma coefficients.

Fig. 5 shows cumulative plots of the displacement kerma matrix elements for Si. In this figure the total curve represents the damage due to all cascade sizes. Subsequent curves represent damage in cascades above a certain size. The figure illustrates the fact that threshold effects are observed in the production of the most energetic cascades.

Conclusion

The first contribution presented in this paper is a tabulation of kerma cross sections for Si, which constitutes a complete revision of the data used in current standard practices. A second contribution is the tabulated kerma cross sections for GaAs. These two tabulations are intended to be immediately useful to the radiation hardness testing community.

The distribution of damage configurations or displacement cascade sizes, or alternatively, the displacement damage kerma matrix elements computed in this paper, is a prerequisite to the further study of cascade size effects. The presentation of damage kerma in the (matrix) multigroup format chosen here is a novel approach, which makes its use practical. The approach is more effective than the tabulation of PKA spectra since it is facility-independent and is much more concise, while it includes the cumulative effects of all relevant reaction channels. The theory presented here is a contribution to the still incomplete task of correlating microscopic radiation damage configurations with observed macroscopic effects. The tabulated displacement kerma cross-section matrices for Si and GaAs allow the computation of effective damage coefficients, provided the macroeffectiveness factors can be established by theoretical or experimental means (i.e., by comparison of experiments in various fields).

APPENDIX

TABULATED RESULTS

TABLE I
TOTAL DISPLACEMENT KERMA CROSS SECTIONS

GRP	ENERGY	Si	GaAs	GRP	ENERGY	Si	GaAs	GRP	ENERGY	Si	GaAs	GRP	ENERGY	Si	GaAs
1	1.000-4	1.542+3	6.371+3	52	1.350-3	4.203+2	1.942+3	103	1.900-2	1.118+2	7.459+2	154	2.550-1	3.064+1	3.931+2
2	1.050-4	1.507+3	6.235+3	53	1.425-3	4.093+2	1.901+3	104	2.000-2	1.090+2	7.348+2	155	2.700-1	2.995+1	3.894+2
3	1.100-4	1.471+3	6.094+3	54	1.500-3	3.968+2	1.854+3	105	2.100-2	1.065+2	7.238+2	156	2.800-1	2.913+1	3.851+2
4	1.150-4	1.440+3	5.959+3	55	1.600-3	3.849+2	1.807+3	106	2.200-2	1.040+2	7.135+2	157	3.000-1	2.814+1	3.796+2
5	1.200-4	1.403+3	5.817+3	56	1.700-3	3.738+2	1.765+3	107	2.300-2	1.018+2	7.045+2	158	3.200-1	2.727+1	3.745+2
6	1.275-4	1.363+3	5.654+3	57	1.800-3	3.631+2	1.726+3	108	2.400-2	9.918+1	6.938+2	159	3.400-1	2.641+1	3.698+2
7	1.350-4	1.329+3	5.499+3	58	1.900-3	3.540+2	1.693+3	109	2.550-2	9.639+1	6.820+2	160	3.600-1	2.570+1	3.650+2
8	1.425-4	1.294+3	5.368+3	59	2.000-3	3.451+2	1.659+3	110	2.700-2	9.425+1	6.729+2	161	3.800-1	2.500+1	3.606+2
9	1.500-4	1.254+3	5.217+3	60	2.100-3	3.368+2	1.626+3	111	2.800-2	9.168+1	6.639+2	162	4.000-1	2.434+1	3.558+2
10	1.600-4	1.217+3	5.061+3	61	2.200-3	3.295+2	1.595+3	112	3.000-2	8.862+1	6.518+2	163	4.250-1	2.370+1	3.506+2
11	1.700-4	1.181+3	4.923+3	62	2.300-3	3.222+2	1.570+3	113	3.200-2	8.591+1	6.402+2	164	4.500-1	2.307+1	3.458+2
12	1.800-4	1.148+3	4.791+3	63	2.400-3	3.140+2	1.540+3	114	3.400-2	8.327+1	6.308+2	165	4.750-1	2.243+1	3.410+2
13	1.900-4	1.119+3	4.675+3	64	2.550-3	3.049+2	1.503+3	115	3.600-2	8.103+1	6.220+2	166	5.000-1	2.187+1	3.371+2
14	2.000-4	1.091+3	4.562+3	65	2.700-3	2.981+2	1.475+3	116	3.800-2	7.886+1	6.133+2	167	5.250-1	2.140+1	3.346+2
15	2.100-4	1.064+3	4.460+3	66	2.800-3	2.908+2	1.445+3	117	4.000-2	7.665+1	6.043+2	168	5.500-1	2.093+1	3.321+2
16	2.200-4	1.041+3	4.369+3	67	3.000-3	2.811+2	1.407+3	118	4.250-2	7.441+1	5.956+2	169	5.750-1	2.045+1	3.297+2
17	2.300-4	1.018+3	4.279+3	68	3.200-3	2.720+2	1.375+3	119	4.500-2	7.236+1	5.870+2	170	6.000-1	1.999+1	3.271+2
18	2.400-4	9.921+2	4.172+3	69	3.400-3	2.645+2	1.346+3	120	4.750-2	7.049+1	5.789+2	171	6.300-1	1.953+1	3.246+2
19	2.550-4	9.632+2	4.061+3	70	3.600-3	2.570+2	1.318+3	121	5.000-2	6.881+1	5.720+2	172	6.600-1	1.907+1	3.221+2
20	2.700-4	9.418+2	3.971+3	71	3.800-3	2.503+2	1.290+3	122	5.250-2	6.731+1	5.650+2	173	6.900-1	1.864+1	3.196+2
21	2.800-4	9.186+2	3.873+3	72	4.000-3	2.435+2	1.265+3	123	5.500-2	6.582+1	5.582+2	174	7.200-1	1.821+1	3.168+2
22	3.000-4	8.880+2	3.755+3	73	4.250-3	2.362+2	1.237+3	124	5.750-2	6.433+1	5.515+2	175	7.600-1	1.772+1	3.137+2
23	3.200-4	8.594+2	3.650+3	74	4.500-3	2.299+2	1.210+3	125	6.000-2	6.289+1	5.452+2	176	8.000-1	1.730+1	3.111+2
24	3.400-4	8.356+2	3.551+3	75	4.750-3	2.238+2	1.185+3	126	6.300-2	6.151+1	5.385+2	177	8.400-1	1.693+1	3.086+2
25	3.600-4	8.120+2	3.461+3	76	5.000-3	2.183+2	1.164+3	127	6.600-2	6.012+1	5.318+2	178	8.800-1	1.656+1	3.064+2
26	3.800-4	7.905+2	3.378+3	77	5.250-3	2.131+2	1.144+3	128	6.900-2	5.877+1	5.256+2	179	9.200-1	1.620+1	3.042+2
27	4.000-4	7.692+2	3.291+3	78	5.500-3	2.085+2	1.125+3	129	7.200-2	5.746+1	5.194+2	180	9.600-1	1.583+1	3.019+2
28	4.250-4	7.462+2	3.211+3	79	5.750-3	2.043+2	1.108+3	130	7.600-2	5.595+1	5.120+2	181	1.000+0	1.548+1	2.996+2
29	4.500-4	7.262+2	3.132+3	80	6.000-3	1.997+2	1.090+3	131	8.000-2	5.462+1	5.048+2	182	1.050+0	1.514+1	2.971+2
30	4.750-4	7.069+2	3.054+3	81	6.300-3	1.947+2	1.072+3	132	8.400-2	5.347+1	4.975+2	183	1.100+0	1.480+1	2.951+2
31	5.000-4	6.896+2	2.983+3	82	6.600-3	1.902+2	1.056+3	133	8.800-2	5.232+1	4.913+2	184	1.150+0	1.446+1	2.936+2
32	5.250-4	6.733+2	2.924+3	83	6.900-3	1.863+2	1.040+3	134	9.200-2	5.117+1	4.852+2	185	1.200+0	1.405+1	2.918+2
33	5.500-4	6.586+2	2.866+3	84	7.200-3	1.818+2	1.022+3	135	9.600-2	5.001+1	4.794+2	186	1.275+0	1.365+1	2.898+2
34	5.750-4	6.454+2	2.808+3	85	7.600-3	1.769+2	1.001+3	136	1.000-1	4.891+1	4.745+2	187	1.350+0	1.327+1	2.879+2
35	6.000-4	6.310+2	2.750+3	86	8.000-3	1.727+2	9.848+2	137	1.050-1	4.790+1	4.700+2	188	1.425+0	1.290+1	2.861+2
36	6.300-4	6.152+2	2.696+3	87	8.400-3	1.685+2	9.698+2	138	1.100-1	4.689+1	4.656+2	189	1.500+0	1.253+1	2.839+2
37	6.600-4	6.010+2	2.645+3	88	8.800-3	1.646+2	9.548+2	139	1.150-1	4.588+1	4.611+2	190	1.600+0	1.216+1	2.817+2
38	6.900-4	5.888+2	2.594+3	89	9.200-3	1.612+2	9.397+2	140	1.200-1	4.463+1	4.564+2	191	1.700+0	1.180+1	2.796+2
39	7.200-4	5.745+2	2.536+3	90	9.600-3	1.578+2	9.266+2	141	1.275-1	4.341+1	4.507+2	192	1.800+0	1.150+1	2.777+2
40	7.600-4	5.590+2	2.476+3	91	1.000-2	1.543+2	9.129+2	142	1.350-1	4.227+1	4.454+2	193	1.900+0	1.120+1	2.758+2
41	8.000-4	5.457+2	2.423+3	92	1.050-2	1.507+2	8.989+2	143	1.425-1	4.113+1	4.409+2	194	2.000+0	1.094+1	2.739+2
42	8.400-4	5.326+2	2.373+3	93	1.100-2	1.472+2	8.868+2	144	1.500-1	3.994+1	4.363+2	195	2.100+0	1.071+1	2.721+2
43	8.800-4	5.204+2	2.332+3	94	1.150-2	1.441+2	8.745+2	145	1.600-1	3.871+1	4.312+2	196	2.200+0	1.048+1	2.705+2
44	9.200-4	5.095+2	2.291+3	95	1.200-2	1.403+2	8.595+2	146	1.700-1	3.750+1	4.260+2	197	2.300+0	1.024+1	2.688+2
45	9.600-4	4.987+2	2.250+3	96	1.275-2	1.365+2	8.440+2	147	1.800-1	3.649+1	4.215+2	198	2.400+0	9.960+0	2.668+2
46	1.000-3	4.877+2	2.204+3	97	1.350-2	1.328+2	8.291+2	148	1.900-1	3.550+1	4.173+2	199	2.550+0	9.682+0	2.645+2
47	1.050-3	4.766+2	2.159+3	98	1.425-2	1.291+2	8.145+2	149	2.000-1	3.464+1	4.130+2	200	2.700+0	9.465+0	2.626+2
48	1.100-3	4.655+2	2.122+3	99	1.500-2	1.254+2	8.007+2	150	2.100-1	3.390+1	4.092+2	201	2.800+0	9.208+0	2.605+2
49	1.150-3	4.556+2	2.085+3	100	1.600-2	1.216+2	7.854+2	151	2.200-1	3.316+1	4.055+2	202	3.000+0	8.893+0	2.577+2
50	1.200-3	4.439+2	2.039+3	101	1.700-2	1.180+2	7.708+2	152	2.300-1	3.243+1	4.019+2	203	3.200+0	8.610+0	2.551+2
51	1.275-3	4.313+2	1.985+3	102	1.800-2	1.148+2	7.579+2	153	2.400-1	3.152+1	3.980+2	204	3.400+0	8.332+0	2.525+2

TABLE I (*Continued*)

GRP	ENERGY	Si	GaAs	GRP	ENERGY	Si	GaAs	GRP	ENERGY	Si	GaAs	GRP	ENERGY	Si	GaAs
205	3.600+0	8.098+0	2.499+2	260	6.000+1	1.997+0	2.007+2	315	9.600+2	1.112+2	3.272+2	370	1.600+4	1.648+3	3.058+3
206	3.800+0	7.872+0	2.473+2	261	6.300+1	1.951+0	1.956+2	316	1.000+3	1.163+2	3.129+2	371	1.700+4	1.732+3	3.205+3
207	4.000+0	7.656+0	2.446+2	262	6.600+1	1.906+0	1.989+2	317	1.050+3	1.221+2	3.147+2	372	1.800+4	1.814+3	3.352+3
208	4.250+0	7.454+0	2.416+2	263	6.900+1	1.862+0	2.097+2	318	1.100+3	1.278+2	6.406+2	373	1.900+4	1.890+3	3.499+3
209	4.500+0	7.252+0	2.387+2	264	7.200+1	1.819+0	2.339+2	319	1.150+3	1.336+2	3.136+2	374	2.000+4	1.966+3	3.645+3
210	4.750+0	7.050+0	2.358+2	265	7.600+1	1.770+0	2.791+2	320	1.200+3	1.408+2	3.116+2	375	2.100+4	2.042+3	3.793+3
211	5.000+0	6.873+0	2.338+2	266	8.000+1	1.727+0	3.555+2	321	1.275+3	1.495+2	1.851+3	376	2.200+4	2.110+3	3.939+3
212	5.250+0	6.723+0	2.326+2	267	8.400+1	1.690+0	5.114+2	322	1.350+3	1.582+2	5.061+2	377	2.300+4	2.174+3	4.086+3
213	5.500+0	6.574+0	2.314+2	268	8.800+1	1.653+0	1.995+3	323	1.425+3	1.669+2	1.375+3	378	2.400+4	2.254+3	4.266+3
214	5.750+0	6.424+0	2.302+2	269	9.200+1	1.617+0	6.248+3	324	1.500+3	1.770+2	4.478+2	379	2.550+4	2.356+3	4.456+3
215	6.000+0	6.281+0	2.290+2	270	9.600+1	1.580+0	8.983+2	325	1.600+3	1.885+2	1.684+3	380	2.700+4	2.445+3	4.609+3
216	6.300+0	6.144+0	2.277+2	271	1.000+2	1.545+0	8.842+2	326	1.700+3	2.001+2	6.180+2	381	2.800+4	2.549+3	4.789+3
217	6.600+0	6.007+0	2.264+2	272	1.050+2	1.511+0	7.835+2	327	1.800+3	2.117+2	1.363+3	382	3.000+4	2.682+3	5.031+3
218	6.900+0	5.874+0	2.252+2	273	1.100+2	1.478+0	7.135+2	328	1.900+3	2.232+2	9.020+2	383	3.200+4	2.815+3	5.272+3
219	7.200+0	5.745+0	2.238+2	274	1.150+2	1.444+0	6.938+2	329	2.000+3	2.347+2	6.753+2	384	3.400+4	2.940+3	5.512+3
220	7.600+0	5.598+0	2.222+2	275	1.200+2	1.403+0	6.185+2	330	2.100+3	2.459+2	5.188+2	385	3.600+4	2.987+3	5.752+3
221	8.000+0	5.464+0	2.207+2	276	1.275+2	1.362+0	5.195+2	331	2.200+3	2.572+2	5.318+2	386	3.800+4	3.688+3	5.991+3
222	8.400+0	5.345+0	2.192+2	277	1.350+2	1.325+0	4.444+2	332	2.300+3	2.684+2	5.716+2	387	4.000+4	3.186+3	6.290+3
223	8.800+0	5.226+0	2.177+2	278	1.425+2	1.288+0	3.866+2	333	2.400+3	2.825+2	7.026+2	388	4.250+4	3.003+3	6.649+3
224	9.200+0	5.107+0	2.163+2	279	1.500+2	1.251+0	3.151+2	334	2.550+3	2.992+2	1.433+3	389	4.500+4	2.812+3	7.008+3
225	9.600+0	4.988+0	2.148+2	280	1.600+2	1.214+0	2.469+2	335	2.700+3	3.127+2	1.942+3	390	4.750+4	2.467+3	7.366+3
226	1.000+1	4.878+0	2.137+2	281	1.700+2	1.318+0	2.060+2	336	2.800+3	3.287+2	1.035+3	391	5.000+4	1.843+3	7.728+3
227	1.050+1	4.778+0	2.129+2	282	1.800+2	2.283+0	1.884+2	337	3.000+3	3.502+2	9.304+2	392	5.250+4	1.499+3	8.094+3
228	1.100+1	4.678+0	2.121+2	283	1.900+2	3.401+0	1.828+2	338	3.200+3	3.715+2	6.801+2	393	5.500+4	4.783+4	8.460+3
229	1.150+1	4.578+0	2.113+2	284	2.000+2	5.107+0	1.810+2	339	3.400+3	3.926+2	2.014+3	394	5.750+4	1.142+4	8.826+3
230	1.200+1	4.456+0	2.105+2	285	2.100+2	7.432+0	1.875+2	340	3.600+3	4.137+2	1.351+3	395	6.000+4	7.957+3	9.228+3
231	1.275+1	4.336+0	2.094+2	286	2.200+2	9.757+0	2.018+2	341	3.800+3	4.347+2	2.118+3	396	6.300+4	6.952+3	9.671+3
232	1.350+1	4.225+0	2.084+2	287	2.300+2	1.208+1	2.741+2	342	4.000+3	4.584+2	1.004+3	397	6.600+4	7.159+3	1.011+4
233	1.425+1	4.114+0	2.074+2	288	2.400+2	1.490+1	2.395+3	343	4.250+3	4.856+2	9.885+2	398	6.900+4	6.813+3	1.055+4
234	1.500+1	3.995+0	2.062+2	289	2.550+2	1.716+1	3.406+2	344	4.500+3	5.194+2	1.487+3	399	7.200+4	6.580+3	1.106+4
235	1.600+1	3.870+0	2.050+2	290	2.700+2	1.875+1	3.134+2	345	4.750+3	6.066+2	1.715+3	400	7.600+4	6.296+3	1.164+4
236	1.700+1	3.747+0	2.038+2	291	2.800+2	2.063+1	3.782+2	346	5.000+3	5.804+2	1.631+3	401	8.000+4	6.168+3	1.223+4
237	1.800+1	3.643+0	2.026+2	292	3.000+2	2.404+1	5.539+3	347	5.250+3	6.046+2	1.226+3	402	8.400+4	6.023+3	1.282+4
238	1.900+1	3.541+0	2.014+2	293	3.200+2	2.834+1	5.145+3	348	5.500+3	6.297+2	2.991+3	403	8.800+4	5.829+3	1.341+4
239	2.000+1	3.455+0	2.003+2	294	3.400+2	3.235+1	4.650+2	349	5.750+3	6.548+2	2.109+3	404	9.200+4	5.597+3	1.399+4
240	2.100+1	3.383+0	1.993+2	295	3.600+2	3.442+1	3.891+2	350	6.000+3	6.824+2	2.644+3	405	9.600+4	5.404+3	1.457+4
241	2.200+1	3.311+0	1.984+2	296	3.800+2	3.617+1	3.626+2	351	6.300+3	7.125+2	2.398+3	406	1.000+5	5.183+3	1.517+4
242	2.300+1	3.239+0	1.973+2	297	4.000+2	3.909+1	3.382+2	352	6.600+3	7.426+2	1.421+3	407	1.050+5	4.862+3	1.579+4
243	2.400+1	3.150+0	1.961+2	298	4.250+2	4.322+1	3.553+2	353	6.900+3	7.728+2	1.936+3	408	1.100+5	4.419+3	1.641+4
244	2.550+1	3.055+0	1.947+2	299	4.500+2	4.735+1	8.541+2	354	7.200+3	8.070+2	1.688+3	409	1.150+5	3.971+3	1.703+4
245	2.700+1	2.989+0	1.934+2	300	4.750+2	5.149+1	4.499+2	355	7.600+3	8.447+2	1.748+3	410	1.200+5	3.343+3	1.780+4
246	2.800+1	2.909+0	1.920+2	301	5.000+2	5.524+1	4.915+2	356	8.000+3	8.824+2	2.067+3	411	1.275+5	2.545+3	1.871+4
247	3.000+1	2.812+0	1.902+2	302	5.250+2	5.861+1	6.518+3	357	8.400+3	9.202+2	1.833+3	412	1.350+5	1.865+3	1.963+4
248	3.200+1	2.724+0	1.883+2	303	5.500+2	6.198+1	4.752+2	358	8.800+3	9.579+2	2.262+3	413	1.425+5	1.347+3	2.054+4
249	3.400+1	2.638+0	1.862+2	304	5.750+2	6.535+1	3.711+2	359	9.200+3	9.957+2	2.134+3	414	1.500+5	4.314+3	2.140+4
250	3.600+1	2.565+0	1.842+2	305	6.000+2	6.863+1	3.523+2	360	9.600+3	1.033+3	2.057+3	415	1.600+5	1.901+4	2.222+4
251	3.800+1	2.495+0	1.842+2	306	6.300+2	7.184+1	3.730+2	361	1.000+4	1.073+3	2.047+3	416	1.700+5	6.440+4	2.304+4
252	4.000+1	2.428+0	4.878+2	307	6.600+2	7.505+1	1.825+3	362	1.050+4	1.117+3	2.138+3	417	1.800+5	1.138+5	2.385+4
253	4.250+1	2.365+0	9.162+2	308	6.900+2	7.848+1	4.046+2	363	1.100+4	1.162+3	2.230+3	418	1.900+5	1.110+5	2.466+4
254	4.500+1	2.302+0	4.623+4	309	7.200+2	8.321+1	5.032+3	364	1.150+4	1.207+3	2.308+3	419	2.000+5	9.160+4	2.550+4
255	4.750+1	2.239+0	7.591+3	310	7.600+2	8.872+1	4.512+2	365	1.200+4	1.266+3	2.408+3	420	2.100+5	7.846+4	2.639+4
256	5.000+1	2.183+0	6.666+2	311	8.000+2	9.368+1	8.870+2	366	1.275+4	1.338+3	2.531+3	421	2.200+5	6.957+4	2.727+4
257	5.250+1	2.137+0	4.840+2	312	8.400+2	9.806+1	3.459+2	367	1.350+4	1.410+3	2.653+3	422	2.300+5	6.390+4	2.817+4
258	5.500+1	2.090+0	2.510+2	313	8.800+2	1.024+2	3.294+2	368	1.425+4	1.481+3	2.776+3	423	2.400+5	5.831+4	2.927+4
259	5.750+1	2.043+0	2.252+2	314	9.200+2	1.068+2	1.907+3	369	1.500+4	1.560+3	2.910+3	424	2.550+5	5.482+4	3.046+4

TABLE I (*Continued*)

GRP	ENERGY	Si	GaAs	GRP	ENERGY	Si	GaAs	GRP	ENERGY	Si	GaAs	GRP	ENERGY	Si	GaAs
425	2.700+5	5.243+4	3.142+4	475	3.400+6	1.193+5	1.278+5	525	8.400+6	1.694+5	2.309+5	575	1.340+7	1.828+5	2.553+5
426	2.800+5	5.120+4	3.257+4	476	3.500+6	1.115+5	1.304+5	526	8.500+6	1.683+5	2.307+5	576	1.350+7	1.827+5	2.559+5
427	3.000+5	5.011+4	3.400+4	477	3.600+6	7.012+4	1.346+5	527	8.600+6	1.665+5	2.303+5	577	1.360+7	1.825+5	2.565+5
428	3.200+5	4.912+4	3.531+4	478	3.700+6	1.152+5	1.387+5	528	8.700+6	1.492+5	2.300+5	578	1.370+7	1.823+5	2.570+5
429	3.400+5	4.986+4	3.660+4	479	3.800+6	1.090+5	1.429+5	529	8.800+6	1.621+5	2.296+5	579	1.380+7	1.821+5	2.574+5
430	3.600+5	4.961+4	3.774+4	480	3.900+6	1.344+5	1.470+5	530	8.900+6	1.789+5	2.293+5	580	1.390+7	1.824+5	2.578+5
431	3.800+5	5.199+4	3.886+4	481	4.000+6	1.318+5	1.495+5	531	9.000+6	1.766+5	2.290+5	581	1.400+7	1.836+5	2.584+5
432	4.000+5	5.178+4	4.007+4	482	4.100+6	1.089+5	1.502+5	532	9.100+6	1.570+5	2.288+5	582	1.410+7	1.834+5	2.592+5
433	4.250+5	5.254+4	4.136+4	483	4.200+6	1.643+5	1.509+5	533	9.200+6	1.542+5	2.285+5	583	1.420+7	1.831+5	2.600+5
434	4.500+5	5.339+4	4.263+4	484	4.300+6	1.351+5	1.515+5	534	9.300+6	1.701+5	2.282+5	584	1.430+7	1.829+5	2.608+5
435	4.750+5	5.529+4	4.387+4	485	4.400+6	1.413+5	1.522+5	535	9.400+6	1.742+5	2.278+5	585	1.440+7	1.827+5	2.615+5
436	5.000+5	5.729+4	4.494+4	486	4.500+6	1.388+5	1.527+5	536	9.500+6	1.692+5	2.268+5	586	1.450+7	1.827+5	2.639+5
437	5.250+5	7.773+4	4.583+4	487	4.600+6	1.588+5	1.532+5	537	9.600+6	1.615+5	2.257+5	587	1.460+7	1.829+5	2.680+5
438	5.500+5	1.243+5	4.669+4	488	4.700+6	1.854+5	1.538+5	538	9.700+6	1.679+5	2.249+5	588	1.470+7	1.832+5	2.722+5
439	5.750+5	5.820+4	4.751+4	489	4.800+6	1.608+5	1.542+5	539	9.800+6	1.705+5	2.240+5	589	1.480+7	1.841+5	2.763+5
440	6.000+5	5.251+4	4.857+4	490	4.900+6	1.460+5	1.623+5	540	9.900+6	1.714+5	2.231+5	590	1.490+7	1.851+5	2.804+5
441	6.300+5	5.517+4	4.987+4	491	5.000+6	1.495+5	1.799+5	541	1.000+7	1.742+5	2.243+5	591	1.500+7	1.858+5	2.827+5
442	6.600+5	5.665+4	5.110+4	492	5.100+6	1.703+5	1.818+5	542	1.010+7	1.721+5	2.274+5	592	1.510+7	1.861+5	2.831+5
443	6.900+5	5.918+4	5.251+4	493	5.200+6	1.459+5	1.837+5	543	1.020+7	1.723+5	2.306+5	593	1.520+7	1.864+5	2.834+5
444	7.200+5	6.440+4	5.483+4	494	5.300+6	1.207+5	1.855+5	544	1.030+7	1.740+5	2.337+5	594	1.530+7	1.866+5	2.838+5
445	7.600+5	8.778+4	5.634+4	495	5.400+6	1.176+5	1.874+5	545	1.040+7	1.646+5	2.344+5	595	1.540+7	1.869+5	2.842+5
446	8.000+5	1.365+5	5.727+4	496	5.500+6	1.459+5	1.892+5	546	1.050+7	1.649+5	2.336+5	596	1.550+7	1.872+5	2.844+5
447	8.400+5	7.815+4	5.809+4	497	5.600+6	1.526+5	1.910+5	547	1.060+7	1.662+5	2.329+5	597	1.560+7	1.875+5	2.847+5
448	8.800+5	8.766+4	5.929+4	498	5.700+6	1.798+5	1.928+5	548	1.070+7	1.702+5	2.323+5	598	1.570+7	1.878+5	2.848+5
449	9.200+5	1.113+5	6.305+4	499	5.800+6	1.650+5	1.945+5	549	1.080+7	1.746+5	2.319+5	599	1.580+7	1.887+5	2.851+5
450	9.600+5	1.116+5	6.720+4	500	5.900+6	1.376+5	1.962+5	550	1.090+7	1.720+5	2.376+5	600	1.590+7	1.897+5	2.853+5
451	1.000+6	7.554+4	7.011+4	501	6.000+6	1.533+5	1.971+5	551	1.100+7	1.692+5	2.422+5	601	1.600+7	1.903+5	2.862+5
452	1.100+6	6.255+4	7.162+4	502	6.100+6	1.285+5	1.972+5	552	1.110+7	1.664+5	2.423+5	602	1.610+7	1.906+5	2.880+5
453	1.200+6	8.884+4	7.243+4	503	6.200+6	1.760+5	1.972+5	553	1.120+7	1.706+5	2.426+5	603	1.620+7	1.908+5	2.897+5
454	1.300+6	8.859+4	7.257+4	504	6.300+6	1.508+5	1.972+5	554	1.130+7	1.774+5	2.429+5	604	1.630+7	1.911+5	2.915+5
455	1.400+6	9.877+4	7.835+4	505	6.400+6	1.401+5	1.971+5	555	1.140+7	1.771+5	2.433+5	605	1.640+7	1.914+5	2.932+5
456	1.500+6	1.057+5	8.432+4	506	6.500+6	1.202+5	1.971+5	556	1.150+7	1.806+5	2.437+5	606	1.650+7	1.916+5	2.949+5
457	1.600+6	1.628+5	8.456+4	507	6.600+6	1.518+5	1.970+5	557	1.160+7	1.782+5	2.441+5	607	1.660+7	1.918+5	2.965+5
458	1.700+6	7.816+4	8.806+4	508	6.700+6	1.630+5	1.969+5	558	1.170+7	1.783+5	2.445+5	608	1.670+7	1.919+5	2.982+5
459	1.800+6	1.329+5	9.533+4	509	6.800+6	1.481+5	1.968+5	559	1.180+7	1.785+5	2.450+5	609	1.680+7	1.921+5	2.999+5
460	1.900+6	1.320+5	1.032+5	510	6.900+6	1.430+5	1.967+5	560	1.190+7	1.789+5	2.485+5	610	1.690+7	1.923+5	3.015+5
461	2.000+6	9.528+4	1.052+5	511	7.000+6	1.622+5	1.974+5	561	1.200+7	1.804+5	2.511+5	611	1.700+7	1.923+5	3.023+5
462	2.100+6	1.070+5	1.036+5	512	7.100+6	1.413+5	1.989+5	562	1.210+7	1.805+5	2.510+5	612	1.710+7	1.922+5	3.022+5
463	2.200+6	1.058+5	1.026+5	513	7.200+6	1.718+5	2.004+5	563	1.220+7	1.806+5	2.510+5	613	1.720+7	1.920+5	3.021+5
464	2.300+6	1.031+5	1.030+5	514	7.300+6	1.714+5	2.019+5	564	1.230+7	1.806+5	2.509+5	614	1.730+7	1.919+5	3.020+5
465	2.400+6	1.192+5	1.036+5	515	7.400+6	1.696+5	2.034+5	565	1.240+7	1.807+5	2.507+5	615	1.740+7	1.918+5	3.019+5
466	2.500+6	1.314+5	1.041+5	516	7.500+6	1.649+5	2.049+5	566	1.250+7	1.810+5	2.505+5	616	1.750+7	1.920+5	3.029+5
467	2.600+6	1.159+5	1.045+5	517	7.600+6	1.730+5	2.064+5	567	1.260+7	1.814+5	2.502+5	617	1.760+7	1.925+5	3.050+5
468	2.700+6	1.071+5	1.048+5	518	7.700+6	1.783+5	2.089+5	568	1.270+7	1.819+5	2.503+5	618	1.770+7	1.930+5	3.071+5
469	2.800+6	1.349+5	1.051+5	519	7.800+6	1.790+5	2.174+5	569	1.280+7	1.823+5	2.527+5	619	1.780+7	1.938+5	3.092+5
470	2.900+6	9.890+4	1.138+5	520	7.900+6	1.892+5	2.271+5	570	1.290+7	1.827+5	2.554+5	620	1.790+7	1.950+5	3.113+5
471	3.000+6	1.202+5	1.234+5	521	8.000+6	1.672+5	2.320+5	571	1.300+7	1.830+5	2.567+5	621	1.800+7.		
472	3.100+6	1.314+5	1.245+5	522	8.100+6	1.571+5	2.318+5	572	1.310+7	1.829+5	2.562+5				
473	3.200+6	1.179+5	1.257+5	523	8.200+6	1.614+5	2.315+5	573	1.320+7	1.829+5	2.558+5				
474	3.300+6	1.140+5	1.267+5	524	8.300+6	1.651+5	2.312+5	574	1.330+7	1.828+5	2.553+5				

TABLE II
Si Displacement Kerma Matrix

Neutron Energy Group	range	E_D group 1 range (eV) 0.0 - 5.964E+3	2 1.299E+4	3 2.831E+4	4 6.168E+4	5 1.344E+5	6 1.872E+5	7 2.400E+5
1	1.00E-5	1.341E+2	0.000E+0	0.000E+0	0.000E+0	0.000E+0	0.000E+0	0.000E+0
2	4.14E-1	3.464E+1	0.000E+0	0.000E+0	0.000E+0	0.000E+0	0.000E+0	0.000E+0
3	1.13E+0	2.097E+1	0.000E+0	0.000E+0	0.000E+0	0.000E+0	0.000E+0	0.000E+0
4	3.06E+0	1.199E+1	0.000E+0	0.000E+0	0.000E+0	0.000E+0	0.000E+0	0.000E+0
5	1.07E+1	6.833E+0	0.000E+0	0.000E+0	0.000E+0	0.000E+0	0.000E+0	0.000E+0
6	2.90E+1	3.912E+0	0.000E+0	0.000E+0	0.000E+0	0.000E+0	0.000E+0	0.000E+0
7	1.01E+2	2.056E+1	0.000E+0	0.000E+0	0.000E+0	0.000E+0	0.000E+0	0.000E+0
8	5.83E+2	9.854E+1	0.000E+0	0.000E+0	0.000E+0	0.000E+0	0.000E+0	0.000E+0
9	1.23E+3	2.418E+2	0.000E+0	0.000E+0	0.000E+0	0.000E+0	0.000E+0	0.000E+0
10	3.35E+3	6.817E+2	0.000E+0	0.000E+0	0.000E+0	0.000E+0	0.000E+0	0.000E+0
11	1.03E+4	1.537E+3	0.000E+0	0.000E+0	0.000E+0	0.000E+0	0.000E+0	0.000E+0
12	2.19E+4	2.164E+3	0.000E+0	0.000E+0	0.000E+0	0.000E+0	0.000E+0	0.000E+0
13	2.48E+4	2.748E+3	0.000E+0	0.000E+0	0.000E+0	0.000E+0	0.000E+0	0.000E+0
14	5.25E+4	7.118E+3	1.532E+3	0.000E+0	0.000E+0	0.000E+0	0.000E+0	0.000E+0
15	1.11E+5	8.452E+2	1.936E+3	4.309E+1	0.000E+0	0.000E+0	0.000E+0	0.000E+0
16	1.58E+5	3.313E+3	1.347E+4	3.249E+4	9.249E+3	0.000E+0	0.000E+0	0.000E+0
17	5.50E+5	1.923E+3	6.714E+3	2.499E+4	4.919E+4	2.859E+2	0.000E+0	0.000E+0
18	1.11E+6	8.939E+2	3.342E+3	1.423E+4	4.071E+4	3.825E+4	0.000E+0	0.000E+0
19	1.83E+6	1.036E+3	3.779E+3	1.602E+4	4.701E+4	4.861E+4	0.000E+0	0.000E+0
20	2.31E+6	5.470E+2	2.089E+3	1.088E+4	4.303E+4	4.705E+4	0.000E+0	0.000E+0
21	2.39E+6	5.956E+2	2.296E+3	1.097E+4	4.099E+4	6.302E+4	0.000E+0	0.000E+0
22	3.01E+6	4.673E+2	1.782E+3	7.545E+3	2.811E+4	7.812E+4	6.766E+0	0.000E+0
23	4.07E+6	4.263E+2	1.722E+3	7.602E+3	2.714E+4	9.487E+4	7.946E+3	0.000E+0
24	4.72E+6	5.361E+2	2.077E+3	8.748E+3	2.787E+4	9.966E+4	2.816E+4	0.000E+0
25	4.97E+6	3.283E+2	1.298E+3	5.861E+3	2.234E+4	8.968E+4	2.917E+4	0.000E+0
26	6.38E+6	2.267E+2	8.795E+2	4.276E+3	1.684E+4	8.725E+4	4.026E+4	0.000E+0
27	7.41E+6	2.242E+2	8.739E+2	3.944E+3	1.494E+4	9.185E+4	5.981E+4	0.000E+0
28	8.19E+6	2.302E+2	1.019E+3	4.029E+3	1.424E+4	8.551E+4	6.020E+4	0.000E+0
29	9.05E+6	2.075E+2	7.767E+2	3.472E+3	1.232E+4	8.089E+4	6.768E+4	0.000E+0
30	1.00E+7	2.005E+2	9.027E+2	3.316E+3	1.135E+4	7.516E+4	7.917E+4	1.780E+0
31	1.11E+7	2.135E+2	9.613E+2	3.522E+3	1.142E+4	7.008E+4	8.944E+4	2.108E+2
32	1.22E+7	2.189E+2	8.162E+2	3.466E+3	1.144E+4	6.645E+4	9.659E+4	1.144E+3
33	1.28E+7	2.146E+2	8.027E+2	3.429E+3	1.105E+4	6.191E+4	1.016E+5	2.597E+3
34	1.38E+7	2.093E+2	7.853E+2	3.370E+3	1.074E+4	5.911E+4	1.039E+5	3.674E+3
35	1.42E+7	2.082E+2	7.818E+2	3.358E+3	1.058E+4	5.675E+4	1.063E+5	4.097E+3
36	1.49E+7	2.179E+2	8.199E+2	3.541E+3	1.105E+4	5.338E+4	1.127E+5	5.441E+3
37	1.69E+7	2.185E+2	8.264E+2	3.631E+3	1.161E+4	4.983E+4	1.173E+5	8.032E+3
	1.80E+7							

TABLE III
GaAs Displacement Kerma Matrix

Neutron Energy Group	range	E_D group 1	2	3	4	5	6	7
	range (eV)	0.0 - 6.438E+3	2.018E+4	6.327E+4	1.983E+5	2.924E+5	3.865E+5	4.806E+5
1	1.00E-5	1.018E+3	0.000E+0	0.000E+0	0.000E+0	0.000E+0	0.000E+0	0.000E+0
2	4.14E-1	5.926E+2	0.000E+0	0.000E+0	0.000E+0	0.000E+0	0.000E+0	0.000E+0
3	1.13E+0	5.172E+2	0.000E+0	0.000E+0	0.000E+0	0.000E+0	0.000E+0	0.000E+0
4	3.06E+0	4.390E+2	0.000E+0	0.000E+0	0.000E+0	0.000E+0	0.000E+0	0.000E+0
5	1.07E+1	3.861E+2	0.000E+0	0.000E+0	0.000E+0	0.000E+0	0.000E+0	0.000E+0
6	2.90E+1	5.542E+3	0.000E+0	0.000E+0	0.000E+0	0.000E+0	0.000E+0	0.000E+0
7	1.01E+2	1.777E+3	0.000E+0	0.000E+0	0.000E+0	0.000E+0	0.000E+0	0.000E+0
8	5.83E+2	1.485E+3	0.000E+0	0.000E+0	0.000E+0	0.000E+0	0.000E+0	0.000E+0
9	1.23E+3	1.292E+3	0.000E+0	0.000E+0	0.000E+0	0.000E+0	0.000E+0	0.000E+0
10	3.35E+3	2.056E+3	0.000E+0	0.000E+0	0.000E+0	0.000E+0	0.000E+0	0.000E+0
11	1.03E+4	3.045E+3	0.000E+0	0.000E+0	0.000E+0	0.000E+0	0.000E+0	0.000E+0
12	2.19E+4	4.228E+3	0.000E+0	0.000E+0	0.000E+0	0.000E+0	0.000E+0	0.000E+0
13	2.48E+4	5.962E+3	0.000E+0	0.000E+0	0.000E+0	0.000E+0	0.000E+0	0.000E+0
14	5.25E+4	1.188E+4	0.000E+0	0.000E+0	0.000E+0	0.000E+0	0.000E+0	0.000E+0
15	1.11E+5	1.924E+4	0.000E+0	0.000E+0	0.000E+0	0.000E+0	0.000E+0	0.000E+0
16	1.58E+5	1.105E+4	2.506E+4	3.727E+2	0.000E+0	0.000E+0	0.000E+0	0.000E+0
17	5.50E+5	5.147E+3	2.564E+4	2.789E+4	9.435E+0	0.000E+0	0.000E+0	0.000E+0
18	1.11E+6	2.847E+3	1.598E+4	5.743E+4	2.850E+3	0.000E+0	0.000E+0	0.000E+0
19	1.83E+6	2.292E+3	1.007E+4	6.677E+4	2.375E+4	5.335E+0	0.000E+0	0.000E+0
20	2.31E+6	2.203E+3	9.194E+3	6.412E+4	2.781E+4	2.325E+1	0.000E+0	0.000E+0
21	2.39E+6	2.335E+3	9.476E+3	6.196E+4	3.245E+4	6.060E+1	0.000E+0	0.000E+0
22	3.01E+6	2.448E+3	9.478E+3	5.190E+4	6.811E+4	2.570E+2	0.000E+0	0.000E+0
23	4.07E+6	2.480E+3	1.016E+4	4.559E+4	9.303E+4	6.133E+2	0.000E+0	0.000E+0
24	4.72E+6	2.498E+3	1.071E+4	4.488E+4	9.631E+4	8.624E+2	2.213E+0	0.000E+0
25	4.97E+6	2.464E+3	1.067E+4	3.417E+4	1.393E+5	2.069E+3	2.488E+2	0.000E+0
26	6.38E+6	2.400E+3	1.115E+4	3.256E+4	1.465E+5	4.576E+3	8.404E+2	0.000E+0
27	7.41E+6	2.356E+3	1.118E+4	2.911E+4	1.571E+5	1.393E+4	1.381E+3	0.000E+0
28	8.19E+6	2.309E+3	1.110E+4	2.556E+4	1.685E+5	2.140E+4	1.754E+3	1.111E+2
29	9.05E+6	2.248E+3	1.106E+4	2.603E+4	1.633E+5	2.220E+4	1.874E+3	3.741E+2
30	1.00E+7	2.191E+3	1.099E+4	2.421E+4	1.597E+5	3.238E+4	2.072E+3	6.165E+2
31	1.11E+7	2.075E+3	1.061E+4	2.063E+4	1.622E+5	4.612E+4	2.379E+3	8.990E+2
32	1.22E+7	1.949E+3	1.011E+4	1.876E+4	1.669E+5	4.928E+4	2.668E+3	1.142E+3
33	1.28E+7	1.853E+3	9.698E+3	1.749E+4	1.661E+5	5.454E+4	4.580E+3	1.369E+3
34	1.38E+7	1.758E+3	9.259E+3	1.641E+4	1.698E+5	5.414E+4	5.215E+3	1.627E+3
35	1.42E+7	1.705E+3	8.989E+3	1.558E+4	1.696E+5	6.120E+4	6.409E+3	1.725E+3
36	1.49E+7	1.634E+3	8.289E+3	1.282E+4	1.628E+5	8.885E+4	9.794E+3	1.870E+3
37	1.69E+7	1.516E+3	7.442E+3	1.062E+4	1.568E+5	1.111E+5	1.429E+4	2.011E+3
	1.80E+7							

References

[1] M. A. Kirk and L. R. Greenwood, "Determination of the neutron flux and energy spectrum of the primary recoil and damage-energy distributions for materials irradiated in the low temperature fast-neutron facility in CP-5," in *Neutron Transmutation Doping in Semiconductors*, J. M. Meese, Ed. New York: Plenum, 1979, pp. 143–155.

[2] R. E. MacFarlane, D. W. Muir, and F. M. Mann, "Radiation damage calculations with NJOY," *J. Nucl. Mat.*, vols. 122 and 123, pp. 1041–1046, 1984.

[3] R. E. MacFarlane, "NJOY. A code system for producing pointwise and multigroup neutron and photon cross sections from ENDF/B-IV and -V evaluated nuclear data," RSIC, PSR-118, Los Alamos National Laboratory, 1979.

[4] *Annual Book of ASTM Standards*, American Society for Testing and Materials, Philadelphia, PA, vol. 12.02, 1988.

[5] F. L. Vook and H. J. Stein, *Radiation Effects in Semiconductors, Proceedings of the Santa Fe Conference*, F. L. Vook, Ed. New York: Plenum Press, 1968, p. 99.

[6] L. W. Aukerman, *Semiconductors and Semimetals*, vol. 4, R. K. Willardson, Ed. New York: Academic, 1968.

[7] R. S. Averback, R. Benedek, and K. L. Merkle, "Ion-irradiation studies of the damage function of copper and silver," *Phys. Rev.*, vol. B18, p. 4156, Oct. 1978.

[8] B. R. Gossick, "Disordered regions in semiconductors bombarded by fast neutrons," *J. Appl. Phys.*, vol. 30, p. 1214, 1959.

[9] J. H. Crawford, *et al.*, "Nature of bombardment damage and energy levels in semiconductors," *J. Appl. Phys.*, vol. 30, p. 1204, 1959.

[10] V. A. J. van Lint, R. E. Leadon, and J. F. Colwell, "Energy dependence of displacement effects in semiconductors," *IEEE Trans. Nucl. Sci.*, vol. NS-19, no. 6, pp. 181-185, Dec. 1972.

[11] V. V. Verbinski, C. Cassapkis, R. L. Pease, and H. L. Scott, "Simultaneous neutron spectrum and transistor-damage measurements in diverse neutron fields: Validity of DSi(En)," Naval Research Laboratory, Washington, D.C., NRL Memo. Rep. 3929, p. 129, 1979.

[12] G. P. Summers, E. A. Burke, C. J. Dale, E. A. Wolicki, P. W. Marshall, and M. A. Gelhausen, "Correlation of particle induced displacement damage in silicon," *IEEE Trans. Nucl. Sci.*, vol. NS-34, no. 6, pp. 1134-1139, Dec. 1987.

[13] T. F. Luera, J. G. Kelly, H. J. Stein, M. S. Lazo, C. E. Lee, and L. R. Dawson, "Neutron damage equivalence for silicon dioxide, and gallium arsenide," *IEEE Trans. Nucl. Sci.*, vol. NS-34, no. 6, pp. 1557-1563, Dec. 1987.

[14] M. H. Sparks, T. M. Flanders, J. G. Williams, J. G. Kelly, W. W. Sallee, M. Roknizadeh, and J. L. Meason, "Energy dependence of neutron damage in silicon bipolar transistors," *IEEE Trans. Nucl. Sci.*, vol. NS-36, no. 6, pp. 1904-1911, Dec. 1989.

[15] G. P. Mueller and C. S. Guenzer, "Simulations of cascade damage in silicon," *IEEE Trans. Nucl. Sci.*, vol. NS-27, no. 6, pp. 1474-1477, Dec. 1980.

[16] Susan Wood, N. J. Doyle, J. A. Spitznagel, W. J. Choyke, R. M. More, J. N. McGruer, and R. B. Irwin, "Simulation of radiation damage in solids," *IEEE Trans. Nucl. Sci.*, vol. NS-28, no. 6, pp. 4107-4112, Dec. 1981.

[17] G. P. Mueller, N. D. Wilsey, and M. Rosen, "The structure of displacement cascades in silicon," *IEEE Trans. Nucl. Sci.*, vol. NS-29, no. 6, pp. 1493-1497, Dec. 1982.

[18] R. L. Pease, E. W. Enlow, G. L. Dinger, and Paul Marshall, "Comparison of proton and neutron carrier removal rates," *IEEE Trans. Nucl. Sci.*, vol. NS-34, no. 6, pp. 1140-1146, Dec. 1987.

[19] R. N. Hamm, M. L. Rustgi, H. A. Wright, and J. E. Turner, "Energy spectra of heavy fragments from the interaction of protons with communications materials," *IEEE Trans. Nucl. Sci.*, vol. NS-28, no. 6, pp. 4004-4006, Dec. 1984.

[20] G. E. Farrell, P. J. McNulty, and Wagih Abdel-Kader, "Microdosimetric analysis of proton induced reactions in silicon and gallium arsenide," *IEEE Trans. Nucl. Sci.*, vol. NS-31, no. 6, pp. 1073-1077, Dec. 1984.

[21] E. A. Burke, C. J. Dale, A. B. Campbell, G. P. Summers, W. J. Stapor, M. A. Xapsos, T. Palmer, and R. Zuleeg, "Energy dependence of proton induced displacement damage in gallium arsenide," *IEEE Trans. Nucl. Sci.*, vol. NS-34, no. 6, pp. 1220-1226, Dec. 1987.

[22] G. P. Summers, E. A. Burke, M. A. Xapsos, C. J. Dale, P. W. Marshall, and E. L. Petersen, "Displacement damage in GaAs structures," *IEEE Trans. Nucl. Sci.*, vol. NS-35, no. 6, pp. 1221-1226, Dec. 1988.

[23] A. R. Knudson, A. B. Campbell, W. J. Stapor, P. Shapiro, and G. P. Mueller, "Radiation damage effects of electrons and H, He, O, Cl, and Cu ions on GaAs JFETs," *IEEE Trans. Nucl. Sci.*, vol. NS-32, no. 6, pp. 4388-4392, Dec. 1985.

[24] A. B. Campbell, A. R. Knudson, W. J. Stapor, G. Summers, M. A. Xapsos, M. Jessee, T. Palmer, R. Zuleeg, and C. J. Dale, "Particle damage effects in GaAs JFET test structures," *IEEE Trans. Nucl. Sci.*, vol. NS-33, no. 6, pp. 1435-1441, Dec. 1986.

[25] M. T. Robinson, "The energy dependence of neutron radiation damage in solids," in *Nuclear Fusion Reactors, Proc. B.N.E.S. Nuclear Fusion Reactor Conf.*, at Culham Laboratory, Sept. 1969, pp. 363-377, British Nuclear Energy Society, London, 1970.

[26] J. Lindhard, V. Nielsen, M. Scharff, and P. V. Thomsen, "Range concepts and heavy ion ranges (Notes on atomic collisions), *Kgl. Dan Vidensk. Selsk. Mat.-Fys. Medd.*, vol. 33, 1963.

[27] D. E. Cullen and P. K. McLaughlin, "The Lawrence Livermore National Laboratory evaluated nuclear data library in the ENDF-V format," IAEA-NDS-11, Rev. 4, Int. Atomic Energy Agency, Vienna, Austria, 1985.

[28] D. E. Bartine, J. R. Knight, J. V. Pace III, and R. W. Roussin, "Production and testing of the DNA few-group coupled neutron-gamma cross-section library," ORNL/TM-4840 (1977).